American Journal of Engineering Research (AJER)
e-ISSN: 2320-0847 p-ISSN : 2320-0936
Volume-7, Issue-1, pp-88-98
www.ajer.org
Research Paper Open Access

Cyclic Load Behavior of Self-Centering Hammer-Head Bridge Piers

Dina M. Fathi[1], Hussein O. Okail[2], Hesham A. Mahdi[3] and Amr A. Abdelrahman[4]

[1]Teaching Assistant, Structural Engineering and Construction Management Department, Future University in Egypt (FUE), Cairo, Egypt.
[2]Associate Professor, Structural Engineering Department, Ain Shams University, Cairo, Egypt.
[3]Minister of Transportation, Egyptian Ministry of Transportation, Cairo, Egypt.
[4]Head of Structural Engineering Department, Ain Shams University, Cairo, Egypt.

ABSTRACT:*This paper presents an experimental investigation in the cyclic load response of hammer-head bridge piers. The paper investigates the response of piers made of precast elements assembled with unbonded prestressing to provide self-centering capabilities under extreme lateral loading. This technique is beneficial in terms of limiting the expected residual deformations after major seismic events.*
Five one-fifth scale pier prototypes were designed, fabricated and tested under both gravity and lateral cyclic loading in displacement control. The test matrix was designed to investigate the effect of the construction method (monolithic versus precast), level of initial prestressing in the unbonded tendons and the use of energy dissipation rebar to result in fatter hysteresis loops.
Experimental results showed that the proposed construction method is indeed capable of enhancing the cyclic load response characteristics in terms of increased ultimate lateral load capacity, reduced residual displacements, delayed damage states and reasonable energy dissipation capacity. The paper serves as a foundation for the next phase of the research program in which a detailed numerical simulation study will be developed to examine various design considerations related to the seismic behavior of such construction method.

Keywords - *Bridge Piers, Energy Dissipation, Hammer head, Self-Centering, Seismic Behavior.*

Date of Submission: 26-12-2017 Date of acceptance: 11-01-2018

I. INTRODUCTION AND BACKGROUND FOUNDATION

Accelerated Bridge Construction (ABC) is gaining increased attention in bridge engineering community. Major advantages of using ABC system include; reduction of traffic disruption specially in urban settings where traffic control for large periods cannot be permitted while maintaining construction quality and reducing life-cycle costs. Assemblages of bridge elements with post-tensioning tendons result in numerous structural advantages. The system is kept as a single unite during a seismic event achieving less residual displacements by enforcing bridge pier to re-center. Furthermore, the use of post-tensioning increases the level of structural durability of the entire bridge especially for substructures in aggressive environments.

Precast self-centering hammer-head bridge piers have been used in many bridge construction projects in regions of low seismicity. Examples include Mid-Bay Bridge, Louetta Road Overpass in Houston, U.S. Highway 183 elevated in Austin, Tex., Varina-Enon Bridge in Virginia (Billington et al. 1999; Figg and Pate 2004). However, segmental column applications in regions of moderate-to-high seismicity are still limited because of the limited knowledge pertaining to the seismic behavior of such type of bridge pier construction.

In the past few years, some research activities on the seismic behavior of precast self-centering bridge piers have been carried out as (Cohagen et. al., 2008) investigated the effect of variable initial prestressing force on the response of a prestressed column-foundation joint designed to re-center after an earthquake event. It was found that keeping initial prestressing tendons within the proportional limit maximizes the re-centering capability of the bridge bent. Also an increase in the post-tensioning force led to slight increase in damage at high drift ratios [1]. (Yu-Chen Ou et. al., 2010) carried out large-scale experimental program of precast segmental unbonded post-tensioned concrete bridge columns for seismic regions with hollow sections. Main variables were ratios of energy dissipation rebar and initial post-tensioning force. Researchers found that existence of energy dissipation rebar ensures ductility. Also specimens without ED bars failed mainly due to P-delta effect and specimens with ED bars failed due to fracture of the ED bars but with larger drift than the specimens without ED bars [2].

(Zhan-Yu Bu1 et. al., 2015) investigated the difference in seismic behavior of precast post-tensioned segmental bridge columns due to variable tendon arrangement, using energy dissipation mild steel bars and bond condition. Test results showed that unbounded tendons with no energy dissipation rebar showed minor cracks with lower residual drift. Variable arrangement of tendons had no significant effect on moment capacity and residual displacement of the proposed connection system [3].

To promote the use of precast bridge columns in regions of high seismicity, five one-fifth scale pier prototypes were designed, fabricated and tested under both gravity and lateral cyclic loading in displacement control in Housing and Building Research Center (HBRC) in Cairo, Egypt. The developed bridge piers adopted concentric unbonded post-tensioning systems to achieve re-centering ability of the proposed. Experimental results of these tests are presented in this study with the aim to evaluate the behavior of developed precast self-centering hammer head bridge piers under lateral loads and present a foundation for an extensive analytical investigation in this research effort.

II. TEST MATRIX

Five one-fifth scale hammer head bridge piers were designed and fabricated; one monolithic specimen and four precast bridge bents. Different parameters were examined to investigate the lateral response of the proposed construction procedure. These parameters are the method of construction, level of initial prestressing force and existence of energy dissipation rebar by extending column main reinforcement into the foundation downward and into the cap-beam upward.

All tested bridge piers had the same geometry as shown in figure 1; bonded reinforcing bars were used for all test specimens with column reinforcement ratio 1.70% that was confined by 8mm diameter smooth bars with pitch 75mm. Configuration of reference monolithic specimen are shown in figure 1(a). Precast self-centering hammer head bridge bents are illustrated in figure 1(b). Details for all specimens are summarized in Table 1.

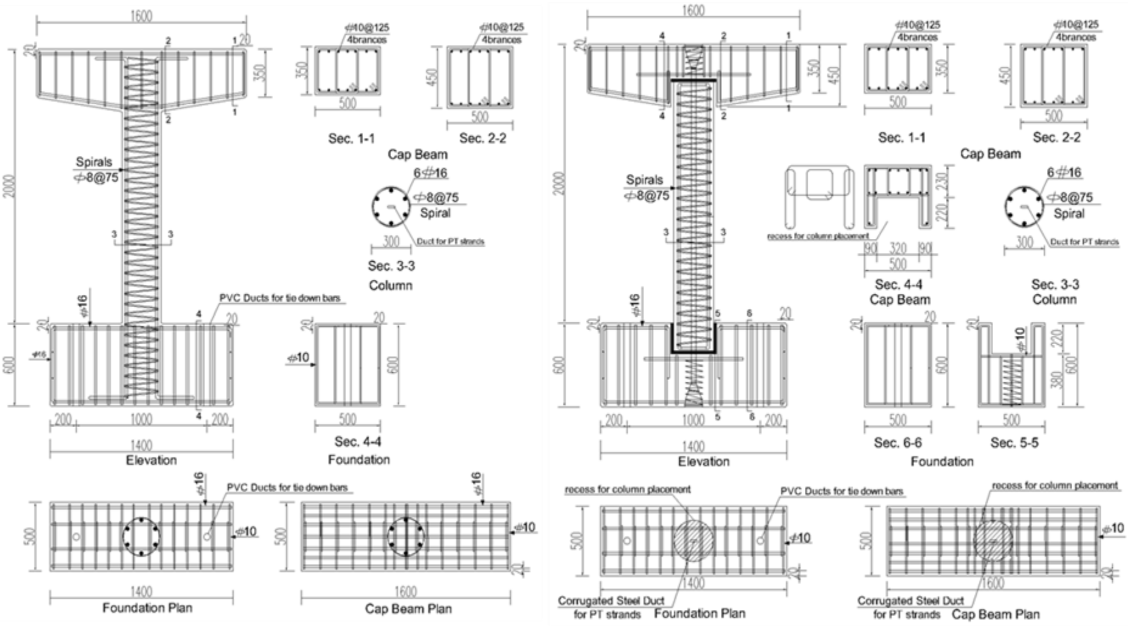

(a) Specimen MN-00-ED

(b) Precast Self-Centering Hammer Head Bridge Bents Specimens Varying in Number of Prestressing Tendons and Addition of ED Bars

Fig. 1 Specimens Dimensions and Details (Dimensions in mm)

Table 1. Test Specimens Details

Specimen	Longitudinal Rebar		Transverse Rebar	Pre-stressing Tendons		ED Rebar*	Construction Type
	RFT	$\%A_g$	Spirals	Tendons	$\% A_g f'_c$	RFT	
MN-00-ED	6 Φ16	1.70%	ϕ8 @ 75mm	--	--	6 Φ 16	Cast in place
PC-30-ED				4 Φ 0.6”	30%	6 Φ16	Pre-Cast
PC-15-ED				2 Φ 0.6”	15%	6 Φ16	Pre-Cast
PC-30				4 Φ 0.6”	30%	--	Pre-Cast
PC-15				2 Φ 0.6”	15%	--	Pre-Cast

*ED Rebar: Energy Dissipation Rebar

III. MATERIAL PROPERTIES

Material properties for concrete and steel reinforcement used for the test specimens were determined experimentally in the materials laboratory at Housing and Building Research Center (HBRC), Egypt. The average strength of concrete based on three tests on unconfined concrete cubes (150×150×150 mm), casted during the pour, is measured at seven days. Also final concrete compressive strength is measured on test day as shown in table 2. Steel reinforcement Φ16, Φ10 and ϕ8 was tested under axial tensile stress, yield and ultimate strength as average of three specimens of each diameter is summarized in Table 3.

Table 2. Average Concrete Strength for Test Specimens

Specimen ID	PC-15-ED	PC-15	PC-30-ED	PC-30	MN-00-ED
Compressive Strength *(MPa)*	37.00	40.20	45.20	44.20	43.10

Table 3. Reinforcing Bar Strength

Bar Diameter (mm)	**Nominal Area (mm^2)**	$f_y(MPa)$	$f_u(MPa)$
8	50.24	368	507
10	78.50	415	669
16	200.96	528	669

IV. TEST SET-UP AND LOADING PROTOCOL

Typical quasi-static test set up was prepared for each tested specimen. All test specimens were fixed in the laboratory floor by two tie down bars and tested using same reacting A-frame. The test configuration is shown in figure 2.

Constant vertical load was applied to each specimen to represent bridge gravity load. Vertical load was chosen as 10% $f_c'.A_g$; that is the minimum value of vertical load from superstructure on a bridge according to AASHTO Guide Specification for LRFD Seismic Bridge Design [4]. To apply lateral cyclic loading in displacement control; each specimen cap beam was fully fixed to the horizontal actuator by four 25mm diameter tie rods. Predefined lateral cyclic displacement pattern was input to Lab View software for all tested specimens are provided in figure 3. Reversed cyclic loading ended when the load carrying capacity went below 85% of the observed peak load at any side (*–ve* push or *+ve* pull) of cyclic displacement. Specimen PC-15 test was only tested to ±80 mm due to short coming in available LVDTs in test day; corresponding load decreased only to 88%.

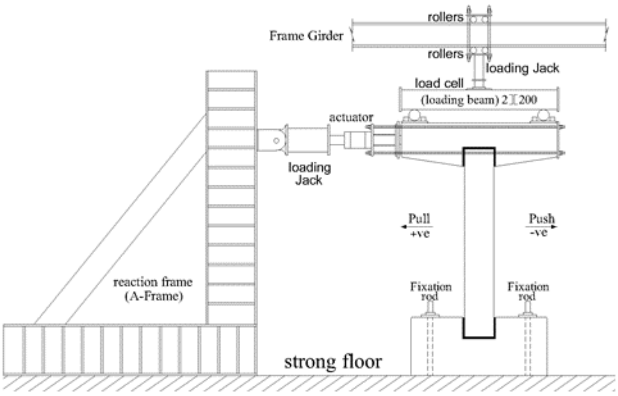

Fig. 2. Test Setup

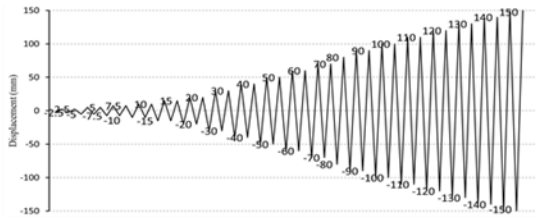

Fig. 3. Lateral Displacement Imposed by Actuator

V. TEST RESULTS AND DISCUSSION

5.1. OBSERVED BEHAVIOR AND FAILURE MODES

Figure 4 shows failure mechanism of all tested specimens at the end of the test. The damage was more in monolithic specimen MN-00-ED and the location of damage was concentrated in the bottom of the column at the plastic hinge zone. General failure propagation in precast self-centering hammer head bridge piers was visually observed as follows: before the maximum compression force was reached, there was some minor cracks, which were flexural cracks perpendicular to the column axis developed in region closed to the specimen foundation. Right after the maximum acting force, cracks increased with increasing lateral displacements. Then, major crack increased suddenly and concrete close to the specimen foundation crushed. Finally, confining stirrups expanded outward and reinforcing bars buckled locally. Specimen PC-30 and PC-15 exhibited similar pattern of damage.

The amount of damage was less as no buckling in reinforcing bars was observed in specimen PC-15 and damage concentrated in the compression side of bridge piers specimens. Specimens with ED bars as in PC-30-ED and PC-15-ED bent in a way that significant cracks did not concentrate in the hinge zone comparing to same specimens without ED bars.

5.2. HYSTERETIC RESPONSE

From the displacement versus force curve in figure 5, it is clear that the hysteretic loops of MN-00ED is larger, exhibiting significant hysteretic energy absorption, and the hysteretic loops of PC-30 and PC-15 are more pinched. Due to the use of ED bars, the strength and the hysteretic energy dissipation of the columns PC-30-ED and PC-15-ED is greatly increased with respect to the traditional monolithic specimen MN-00-ED and same specimens but without energy dissipation rebar as in precast self-centering bridge piers PC-30 and PC-15.

5.3. LATERAL LOAD CAPACITY

Backbone curves can be acquired by connecting all the peak points of every hysteretic curve with smooth curve. Specimens backbone curve in figure 5 (f) shows that most common construction method as in monolithic pier specimen has experienced least ultimate lateral load when compared with precast self-centering bridge piers. The proposed construction method tend to have increased ultimate load in both cases of using energy dissipation rebar or not.

Also extending reinforcing bars into the foundation for energy dissipation purpose raises ultimate load envelop that was clear in specimens PC-30-ED and PC-15-ED when compared with PC-30 and PC-15. Specimens with energy dissipation rebar showed significantly decreasing load as post peak response; PC-30-ED showed 63.58% of ultimate load at +130 mm and specimen PC-15-ED showed 50.52% of ultimate load at +120 mm. Specimens without ED bars showed delay in post peak decreasing load as PC-30 showed 60.34% of ultimate load at -144 mm while almost constant envelop in post peak response at pull side. Specimen PC-15 showed no essentially loss in peak load at both sides till maximum applied displacement.

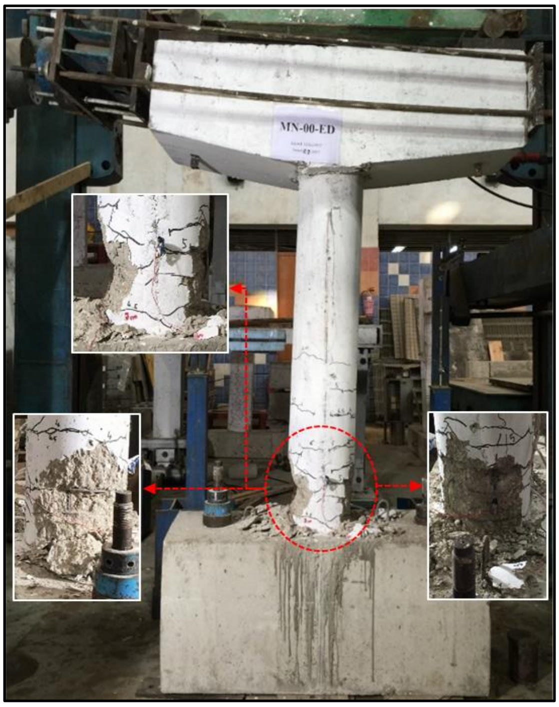

(a) Specimen MN-00-ED at Failure

(b) Specimen PC-30-ED at Failure

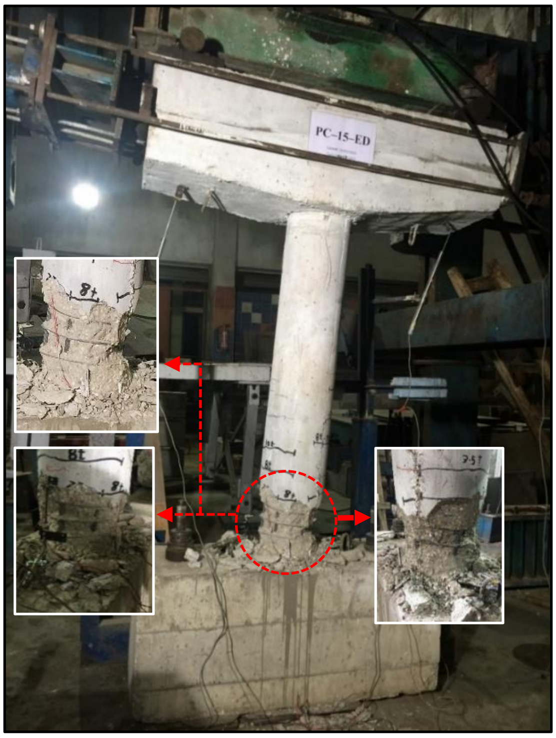

(c) Specimen PC-15-ED at Failure

(d) Specimen PC-30 at Failure

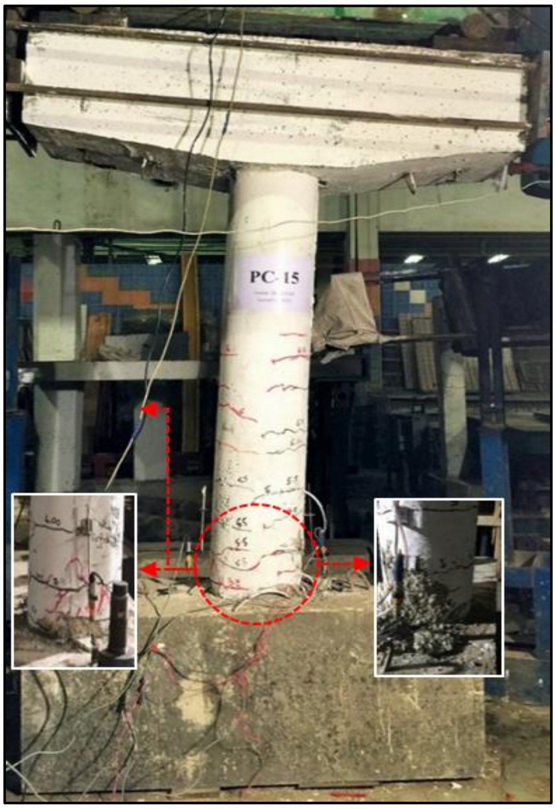

(e) Specimen PC-15 at Failure

Fig. 4. Tested Specimens Failure Mechanisms

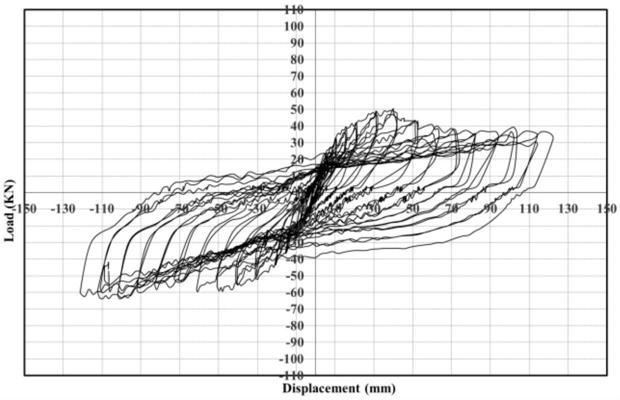

(a) Specimen MN-00-ED

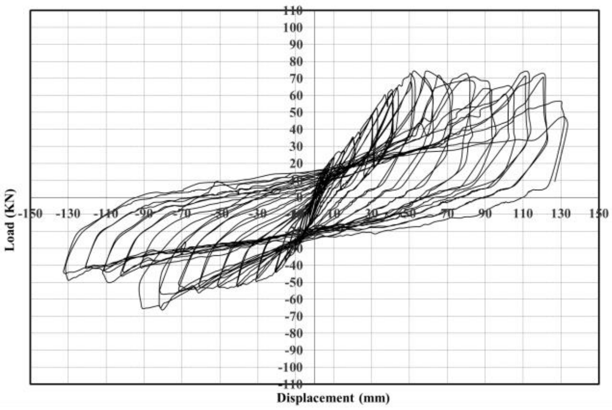

(b) Specimen PC-30-ED

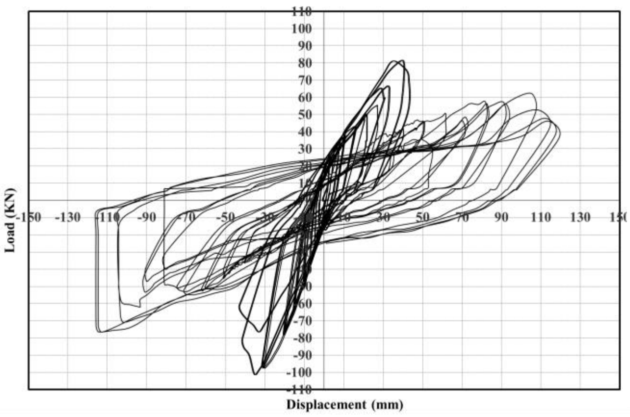

(c) Specimen PC-15-ED

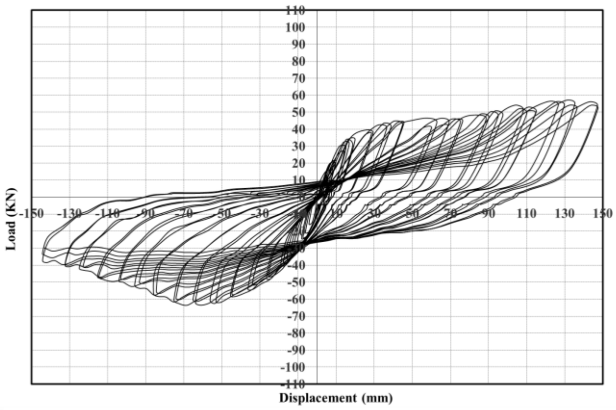

(d) Specimen PC-30

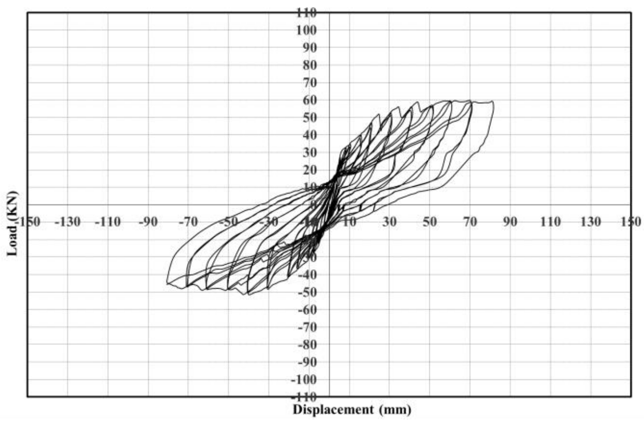

(e) Specimen PC-15

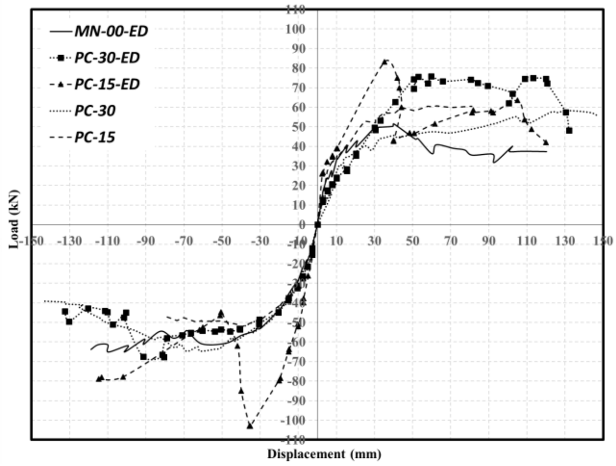

(f) Specimens Backbone Curves

Fig. 5. Specimens Load-Displacement Relationship

Also increasing the prestressing level increases the ultimate load; thus bridge piers with higher level of prestressing exhibited more ductile behavior hence more capability to re-center. As Specimen PC-30-ED reached maximum load at displacements +53 mm and -80 mm while maximum load was reached at +35 mm and -35 mm in specimen PC-15-ED. Also specimen PC-30 reached maximum load at -68 mm and +132 mm while maximum load was reached at -40 mm and +62 mm in case of specimen PC-15.

5.4. SELF-CENTERING CAPABILITIES

To analyze the expected self-centering ability of reinforced concrete bridge piers, Hieber et al. (2005) developed a "re-centering ratio" [5]. This ratio compares the re-centering forces with the resisting forces to determine if the specimen is expected to re-center. The re-centering force consists of the force from the prestressing tendons (P_{pt}) and the axial load (P_{col}), and the resisting force (P_s) comes from the bonded steel reinforcement passing through joints (ED bars) as shown in figure 6; and by summing moments at the centroid of the compression block, the re-centering and resisting moments become:

$$M_{re-centering} = (P_{pt} + P_{col.}).\alpha D \quad (1)$$

$$M_{ressising} = (P_s).\alpha D \quad (2)$$

Thus;

$$\lambda_{re} = \frac{M_{re-centering}}{M_{ressising}} = \frac{P_{col.}+P_{pt}}{P_s} \quad (3)$$

Assuming that prestressing strands have its initial prestressing force and mild steel have yielded; then equation 3 become:

$$\lambda_{re} = \frac{P_{col.}+f_p.A_{p0}}{f_y.A_s} \quad (4)$$

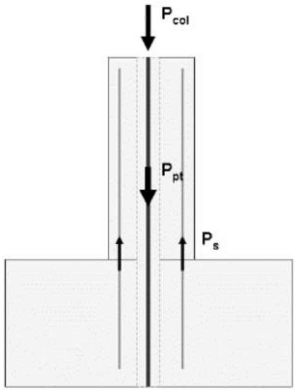

Fig. 6. Counteracting Forces Used to Calculate Re-Centering Ratio [5]

Where; $P_{col.}$ is column vertical load, P_{Pt} is initial prestressing force in strands, f_y is yield strength of the mild steel and αD is distance from column center to the centroid of the concrete compression area.

Table 4 summarizes values of re-centering ratio (λ_{re}) of all tested specimens using equation 4. Re-centering ratio of MN-00-ED is less than one; thus this bridge pier won't re-center. Specimen with energy dissipation rebar PC-30-ED and PC-15-ED had re-centering ratio greater than one which means that these specimens undergoes re-centering behavior.

Bridge piers are expected to undergo large inelastic deformations during severe earthquakes, which can result in permanent or residual displacement. The residual displacement is defined as the displacement of zero-crossing at unloading on the hysteresis loop from the maximum displacement. These residual displacements are important measure of post-earthquake functionality in bridges, and can determine whether or not a bridge remain usable following an earthquake event. Percentage of residual displacement after each cyclic displacement is shown in figure 7. Specimens of precast self-centering construction method achieved less residual displacement through most cycles as shown in figure 7 (a) and (b). Increasing level of prestressing reduced residual displacement that was clear in –ve displacements half cycles as shown in figure 7 (c) and (d). Pull side (+ve) had not accurate residual displacements of specimen PC-30-ED and PC-30 because of the effect of high rigidity of specimen especially at such high level of prestressing. While using energy dissipation rebar, reduces piers re-centering capabilities as shown in figure 7 (e) and (f). The specimen MN-00-ED displayed significant residual displacements. These displacements were almost equal to the peak displacement, meaning small elastic recovery. In contrast, the specimen PC-30 and PC-15 showed the least residual displacements.

Table 4. Re-centering Ratio of Tested Specimens

Specimen	MN-00-ED	PS-30-ED	PC-15-ED	PC-30	PC-15
P_{col}	10 % $A_g.f_c'$				
P_{Pt}	---	30 % $A_g.f_c'$	15 % $A_g.f_c'$	30 % $A_g.f_c'$	15 % $A_g.f_c'$
A_s	6ϕ16	6ϕ16	6ϕ16	---	---
λ_{re}	0.553	2.30	1.45	∞	∞

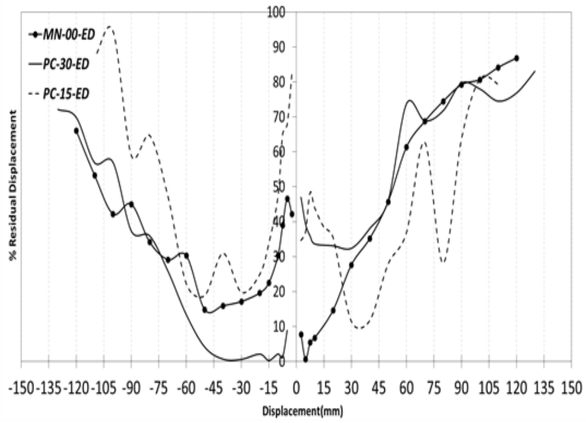

(a) Effect of Construction Method on Residual Displacement of Specimens with ED Rebar

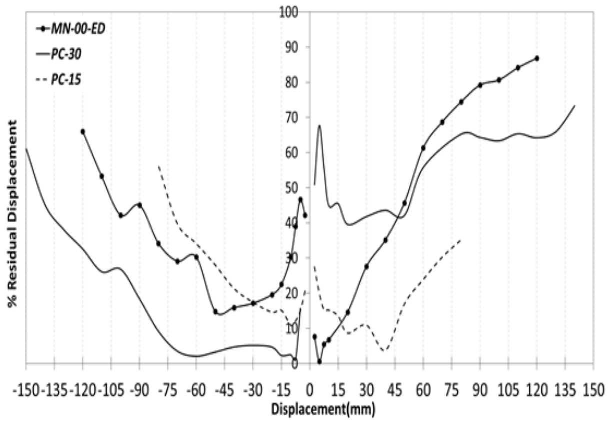

(b) Effect of Construction Method on Residual Displacement of Specimens without ED Rebar

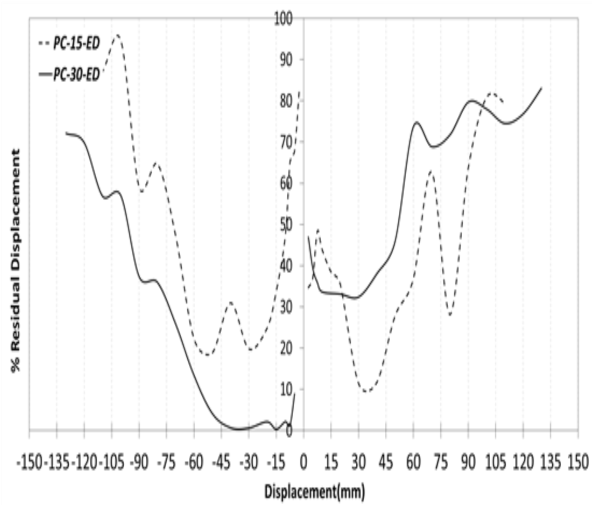

(c) Effect of Prestressing Level on Residual Displacement of Specimens with ED Rebar

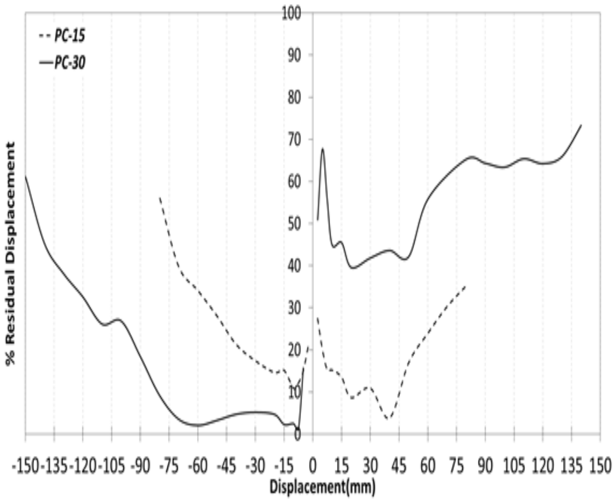

(d) Effect of Prestressing Level on Residual Displacement of Specimens without ED Rebar

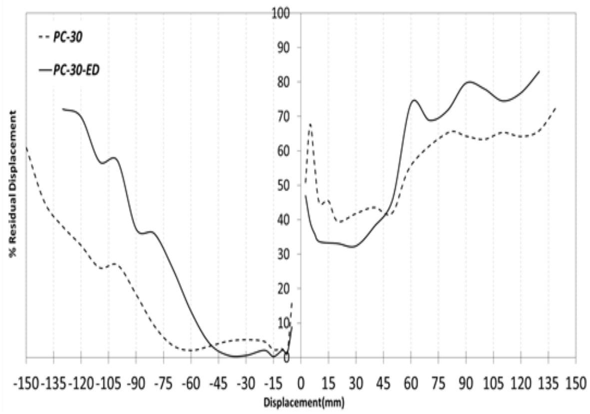

(e) Effect of Using ED Rebar on Residual Displacement of Specimens with ED Rebar

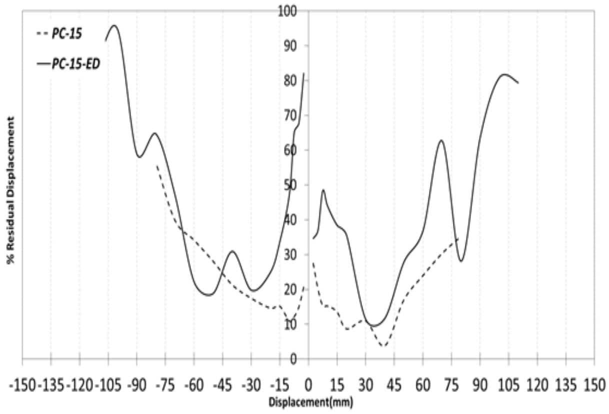

(f) Effect of Using ED Rebar on Residual Displacement of Specimens without ED Rebar

Fig. 7. Comparison of Residual Displacements

5.5. ENERGY DISSIPATION

The energy dissipated during the tests was a measure of the effective damping during an earthquake. The energy dissipated during each cycle is equivalent to the area inside the force-displacement curve. It was calculated per cycle, and then the results for all cycles are added to find the cumulative energy dissipation. The energy per cycle was calculated by using the trapezoidal integration procedure given in equation 5, and it is demonstrated with figure 8.

$$\boldsymbol{E.D._{cycle}} = \sum_i \frac{F_{i+1}+F_i}{2} \cdot (\Delta_{i+1} - \Delta_i) \qquad (5)$$

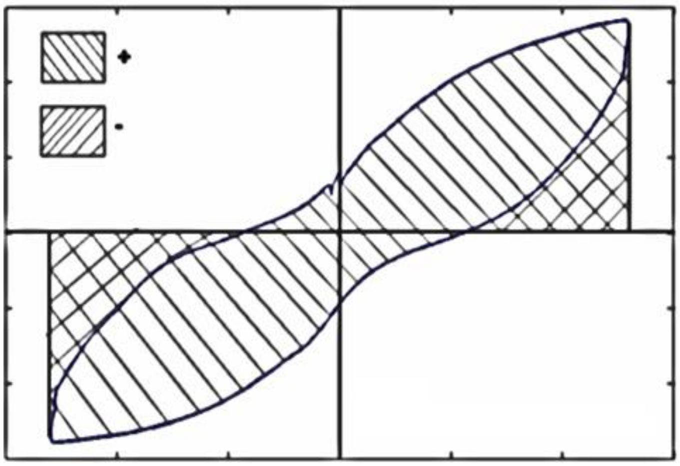

Fig. 8. Example of Energy Dissipation Calculations for One Cycle

All specimens' cumulative dissipated energy was calculated using equation 5; comparison between dissipated energy in each specimen is illustrated in figure 9. As expected monolithic specimens had the largest dissipated energy followed by specimens with energy dissipation rebar PC-30-ED and PC-15-ED and finally comes specimens assembled only with post-tensioned strands PC-30 and PC-15.

Figure 9 (c) and (d) show that specimens with energy dissipation rebar as in specimens PC-30-ED and PC-15-ED showed more energy dissipation than same specimens without energy dissipation rebar as in specimens PC-30 and PC-15. Specimens with higher level of presetressing as in specimens PC-30 and PC-30-ED showed higher energy dissipation as shown in figures 9 (e) and (f) when compared with similar specimens with lower level of prestressing. The effect of using energy dissipation rebar was more significant than increasing level of prestressing; as dissipated energy in specimens with energy rebar increased to more than 50% through most cycles, specimens with higher prestressing level showed no significant increase in dissipated energy when compared with the same specimens with half level of prestressing.

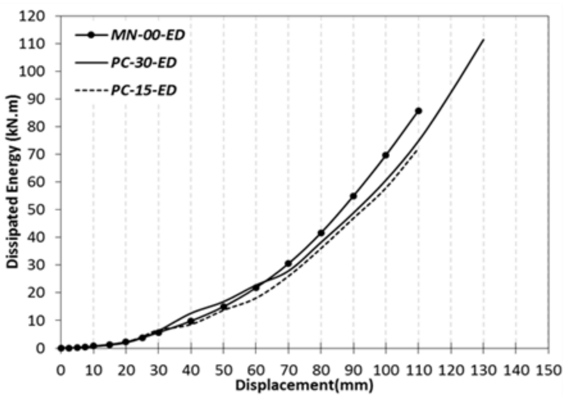

(a) Effect of Construction Method on ED of Specimens with ED Rebar

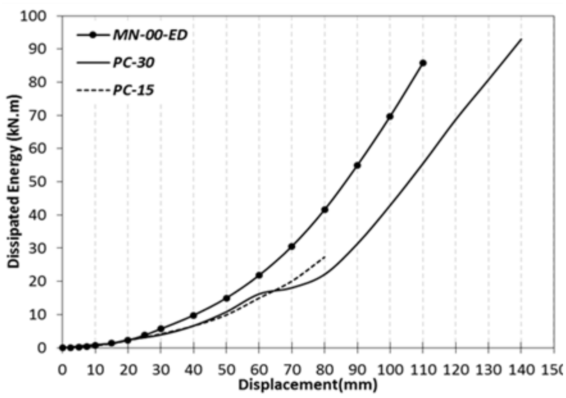

(b) Effect of Construction Method on ED of Specimens without ED Rebar

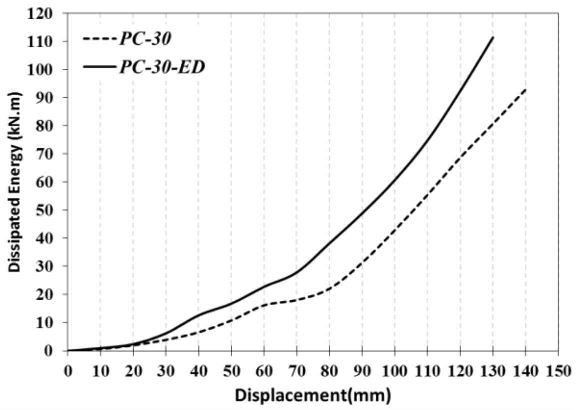

(c) Effect of Using ED Rebar on ED of Specimens with 30% Prestressing Level

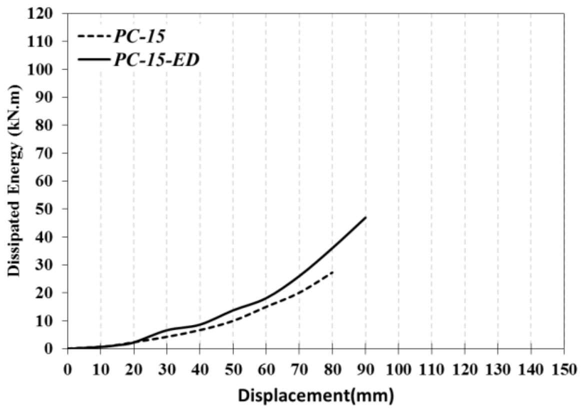

(d) Effect of Using ED Rebar on ED of Specimens with 15% Prestressing Level

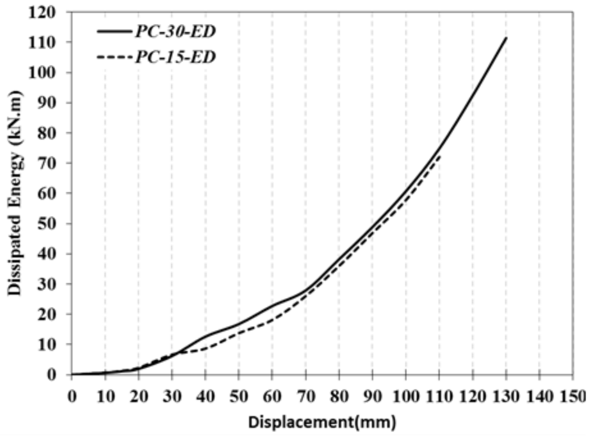

(e) Effect of Prestressing Level on ED of Specimens with ED Rebar

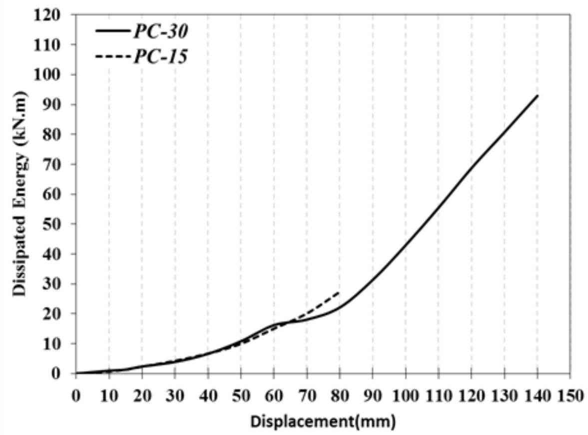

(f) Effect of Prestressing Level on ED of Specimens without ED Rebar

Fig. 9. Cumulative Dissipated Energy at Each Cycle of tested Specimens

VI. CONCLUSIONS

This paper presents an experimental investigation in the cyclic load response of self-centering hammer-head bridge piers using a set of one-fifth scale pier specimens. The following are the key findings for this research effort:

1. The use of hysteretic energy dissipation rebar leads to a significant increase in the lateral strength of the piers. Increases up to 96.50% were observed in specimens with energy dissipation rebar. On the other hand the residual displacement increased significantly. Residual displacements up to 70% of the applied displacement were observed in case of using energy dissipation rebar.
2. The addition of energy dissipation rebar crossing the joint resulted in much higher hysteretic energy dissipation due to plastic deformation of the ED rebar. In case of using energy dissipation rebar; the dissipated energy exceeded 50% when compared with specimens without ED rebar in case of specimens with 30% initial prestressing and 40% in case of specimens with 15% initial prestressing.
3. Although the level of prestressing force does not significantly affect the lateral strength of the piers, it clearly increases the displacement level at which this ultimate strength is achieved. Furthermore, the increase in the level of initial prestressing leads to a significant reduction in the residual displacement.
4. Specimens of the precast self-centering construction method generally achieved less residual displacement through most cycles when compared with traditional monolithic construction method even when using energy dissipation re-bars. Monolithic bridge piers achieved a re-centering ratio less than one, while self-centering specimens achieved re-centering ratios ranging from 1.45 to 2.30 with 15% and 30% initial prestressing, respectively.

5. In general, precast self-centering construction method may be viewed as a viable alternative to traditional monolithic construction in seismically active regions as the system poses desirable structural merits necessary for these regions. In this respect, the reduction in residual displacement and increased displacement tolerances at ultimate load levels are of high degree of structural importance.

ACKNOWLEDGEMENTS

This experimental work has been conducted in reinforced concrete laboratory in Housing and building Research Center in Cairo (HBRC) as a part of Ph.D. thesis. The authors are greatly acknowledged the partial financial support provided by STRAND for POSTTENSIONING TECHNOLOGY to conduct this research.

REFERENCES

[1]. Laila S. Cohagen, Jason B.K. Pang, John F. Stanton and Marc O Eberhard, “A Precast Concrete Bridge Bent Designed to Re-center after an Earthquake”, University of Washington, Washington 2008.
[2]. Yu-Chen Ou, Ping-Hsiung Wang, Mu-Sen Tsai, Kuo-Chun Chang, and George C. Lee, “Large-Scale Experimental Study of Precast Segmental Unbonded Posttensioned Concrete Bridge Columns for Seismic Regions”, Journal of Structural Engineering, 2010.
[3]. Zhan-Yu Bu1, Yu-Chen Ou, Jian-Wei Song, Na-Si Zhang, and George C. Lee, “Cyclic Loading Test of Unbonded and Bonded Posttensioned Precast Segmental Bridge Columns with Circular Section”, Journal of Bridge Engineering, 2015.
[4]. AASHTO (2005). “LRFD Bridge Design Specifications,” 4th edition, American Association of State Highway and Transportation Officials, Washington.
[5]. Phillip M. Davis, Todd M. Janes, Marc O. Eberhard, and John F. Stanton, “Unbonded Pre-Tensioned Columns for Bridges in Seismic Regions”, Pacific Earthquake Engineering Research Center, 2012.
[6]. Mohamed A. ElGawady, and Ahmad Sha’lan, “Seismic Behavior of Self-Centering Precast Segmental Bridge Bents”, *Journal of Bridge Engineering*, 2011.
[7]. Jason B.K. Pang, Kyle P. Steuck, Laila Cohagen, John F. Stanton, and Marc O Eberhard, “Rapidly Constructible Large-Bar Precast Bridge-Bent Seismic Connection”, University of Washington, 2008.
[8]. Mustafa Mashal , Alessandro Palermo, and Zeinab Chegini “Quasi-Static Cyclic Tests Of Half-Scale Fully Precast Bridge Bents Incorporating Emulative And Posttensioned Low Damage Solutions”, *second European conference on earthquake engineering and seismology engineering*, 2014.
[9]. Tae-Hoon Kim, Dai-Jeong Seong, and Hyun Mock Shin, “Seismic Performance Assessment of Hollow Reinforced Concrete and Prestressed Concrete Bridge Columns”, International Journal of Concrete Structures and Materials, 2012.
[10]. Kawashima, K., Une, H., and Sakai, J., “Seismic performance of hollow reinforced concrete arch ribs subjected to cyclic lateral force under varying axial load”, *Journal of Structural Engineering*, 2002.
[11]. Kim, T.-H., Hong, H.-K., Chung, Y.-S., and Shin, H. M., “Seismic performance assessment of reinforced concrete bridge piers with lap splices using shaking table tests”, *Magazine of Concrete Research*, 2009.
[12]. Kim, T.-H., Kim, Y.-J., Kang, H.-T., and Shin, H. M., “Performance assessment of reinforced concrete bridge columns using a damage index”, *Canadian Journal of Civil Engineering*, 2007.
[13]. Kim, T.-H., Lee, K.-M., Yoon, C.-Y., & Shin, H. M., “Inelastic behavior and ductility capacity of reinforced concrete bridge piers under earthquake”, *Journal of Structural Engineering*, 2003.
[14]. Berry, M., and Eberhard, M., “Practical Performance Model for Bar Buckling”, *Journal of Structural Engineering*, 2005.
[15]. Palermo, A., Pampanin, S., and Calvi, G., “Concept and Development of Hybrid Solutions for Seismic Resistant Bridge Systems”, *Journal of Earthquake Engineering*”, 2005.

Dina M. Fathi "Cyclic Load Behavior of Self-Centering Hammer-Head Bridge Piers.”American Journal of Engineering Research (AJER), vol.7, no. 1, 2018, pp. 88-98.